

Wideband Dual-Polarized 1-Bit Unit-cell Design For mmWave RIS

Gabriel G. Machado, M. Ali Babar Abbasi, Adrian
McKernan, Chao Gu, Dmitry Zelenchuk

22nd of March 2024



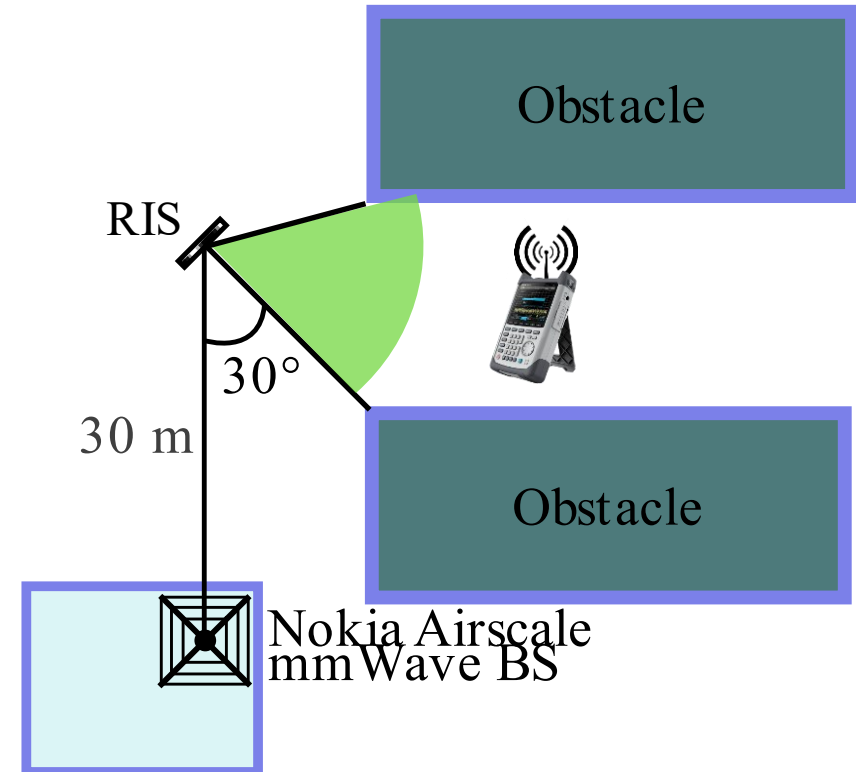
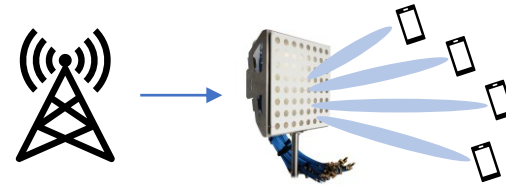
Contents

- Introduction
- Unit-cell model
- Waveguide test
- Pathloss model
- Full RIS simulation
- Experimental results
- Conclusions



Introduction

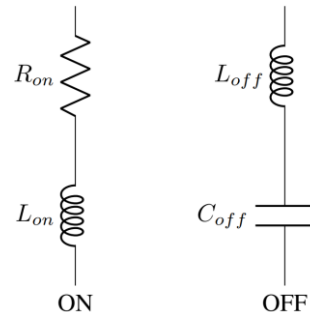
- Millimetre wave communications → LoS
 - Massive MIMO arrays
 - Cell-free networks
 - Distributed antenna systems
- Signals significantly degraded due to:
 - Pathloss
 - Obstacles
 - Buildings
 - Foliage
 - Other people
- Reconfigurable intelligent surfaces (RIS)
 - Dynamically reflect the signal towards UE
 - Potential to significantly improve the energy efficiency of the channel



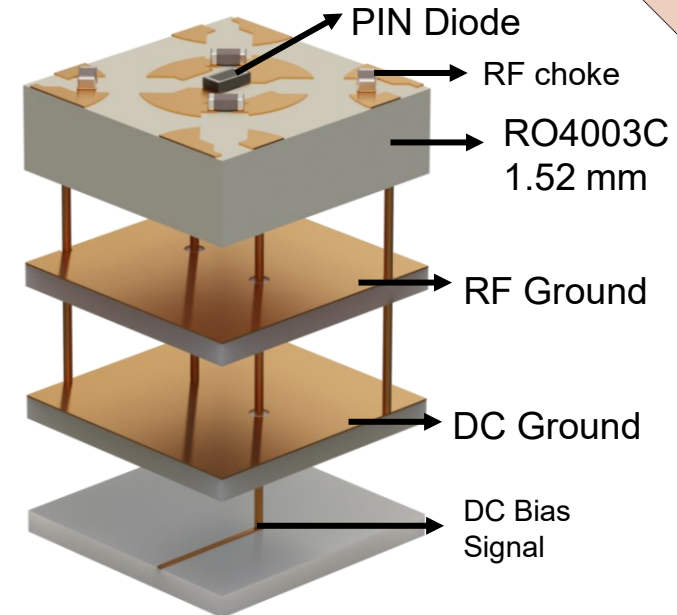
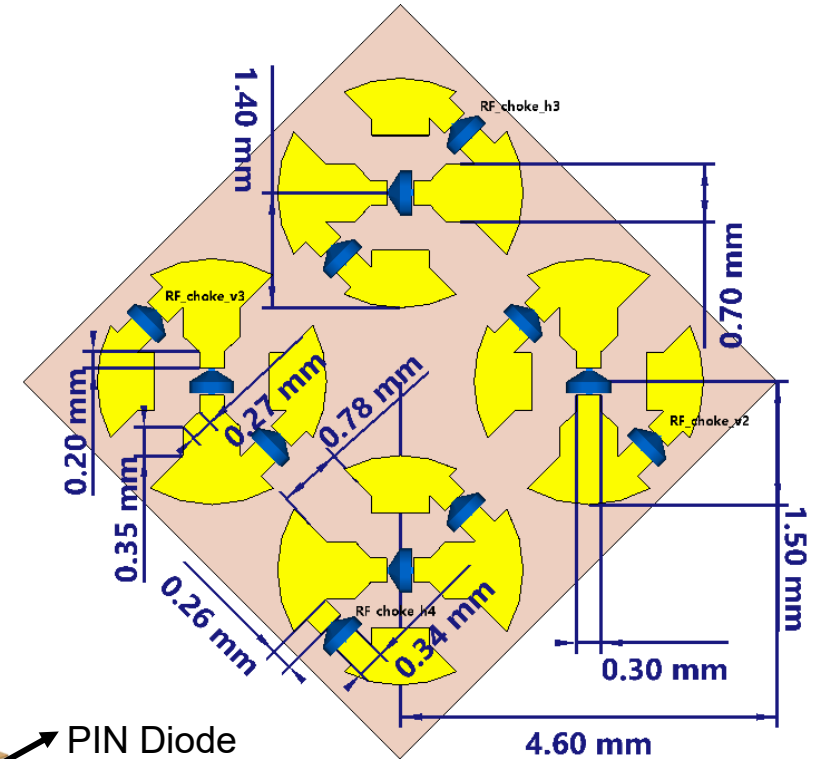
Unit-cell design

- Several design iterations
- Checker-board lattice
 - Contributes to both polarizations
- RF Chokes for bias
- Digitally controlled by p-i-n diodes
 - 1-bit per polarization
- Macom MADP-000907-14020P p-i-n diode

Diode state	L	R	C
On	30 pH	6 Ω	N/A
Off	30 pH	N/A	50 fF



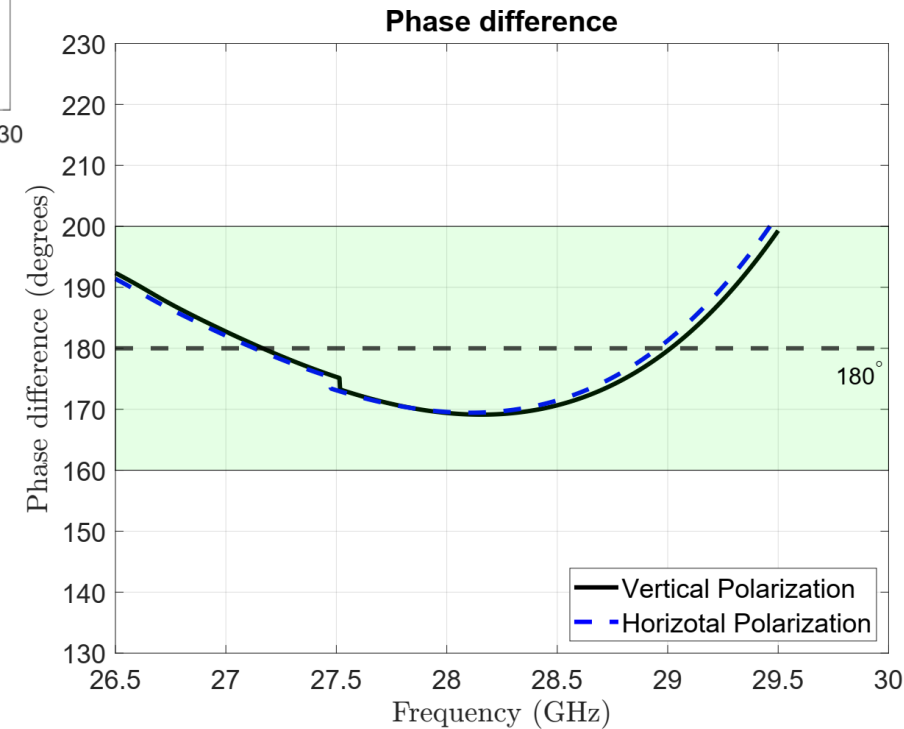
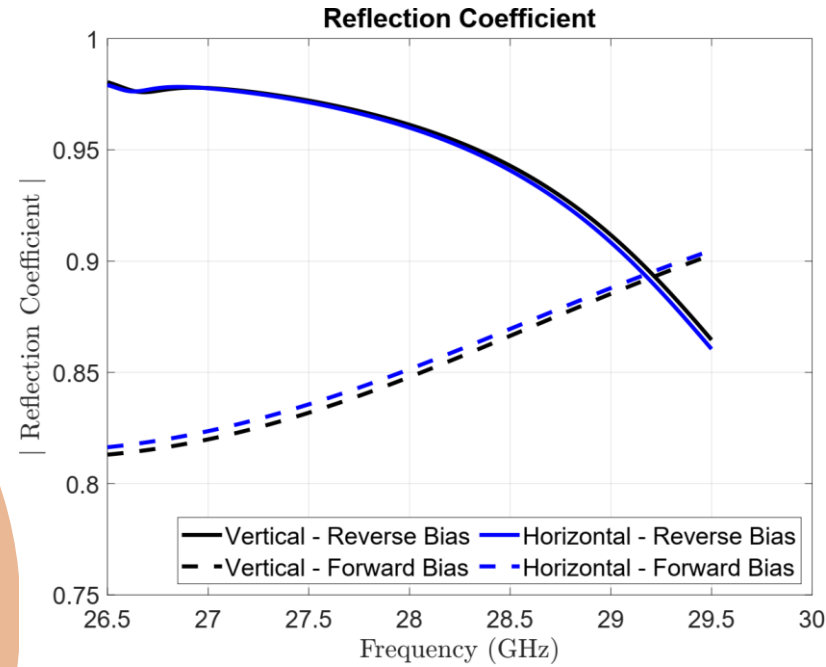
Final iteration



Numerical results

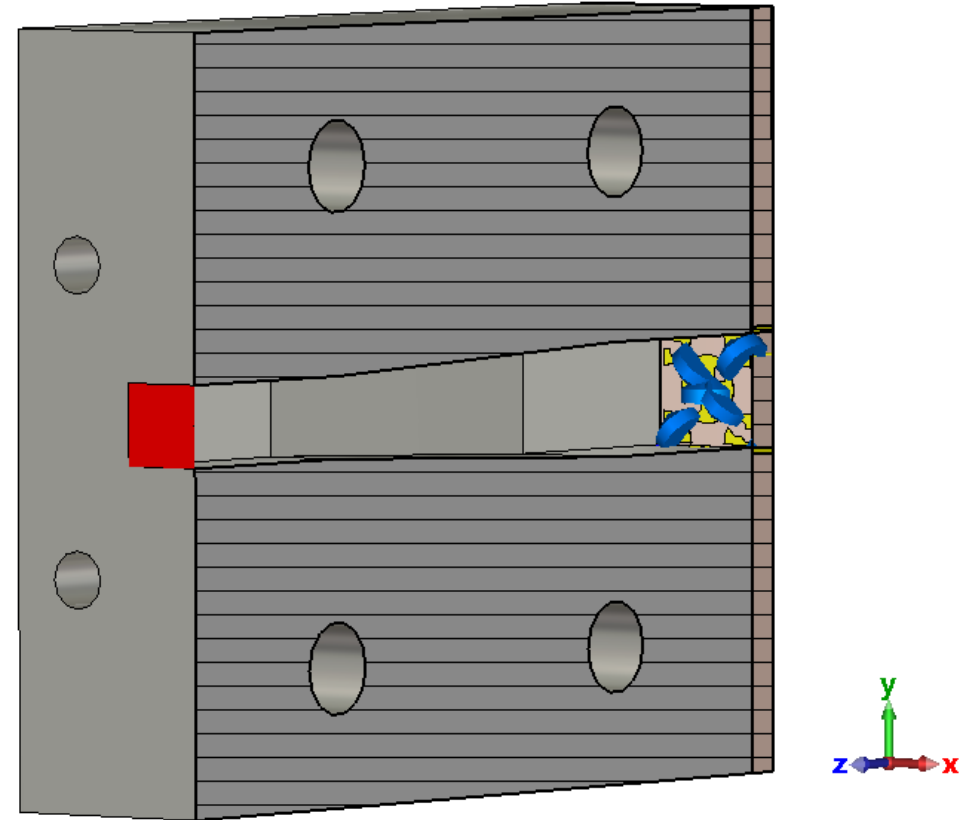
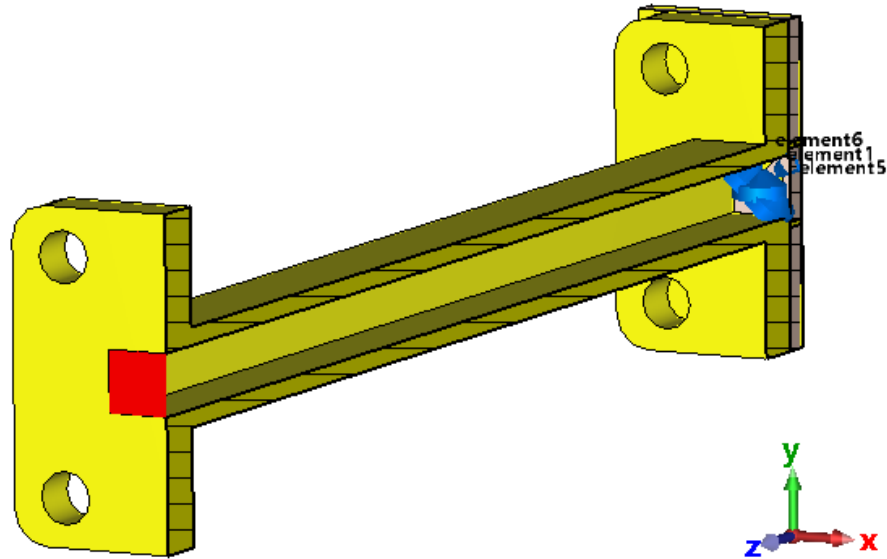
Simulated in CST Microwave Studio

- Floquet ports and periodic boundary
- De-embedded to the surface of the unit-cell
- Optimised for 30° incidence



n257 mmWave band,
n261 in particular

Waveguide tests

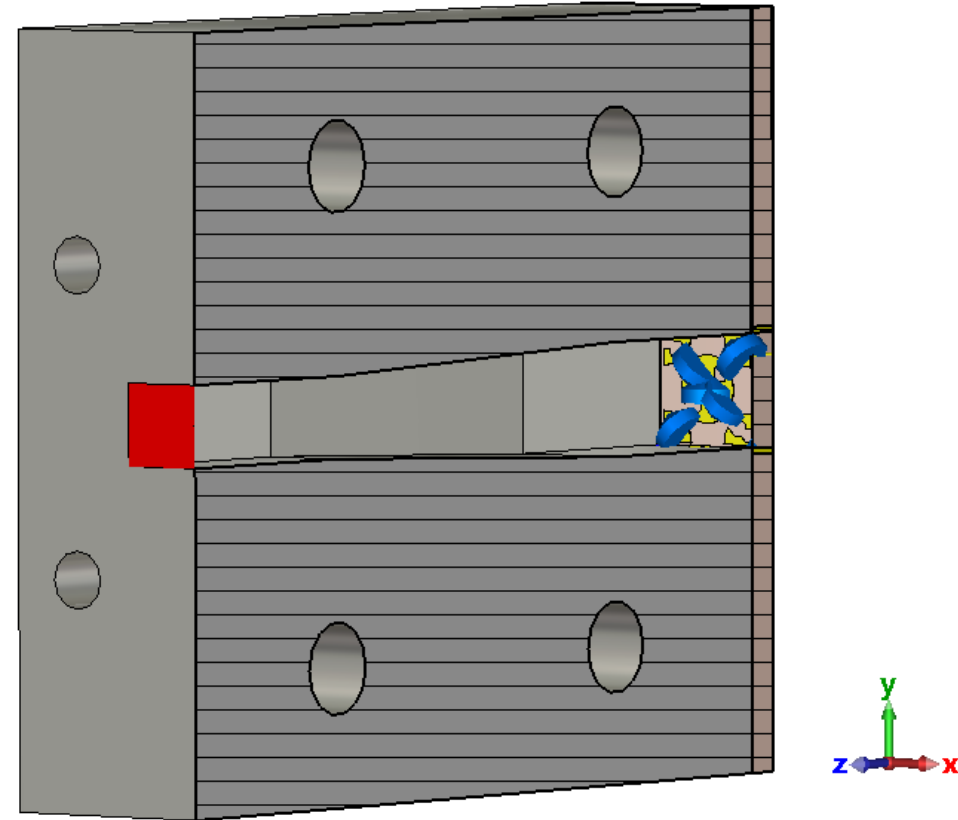
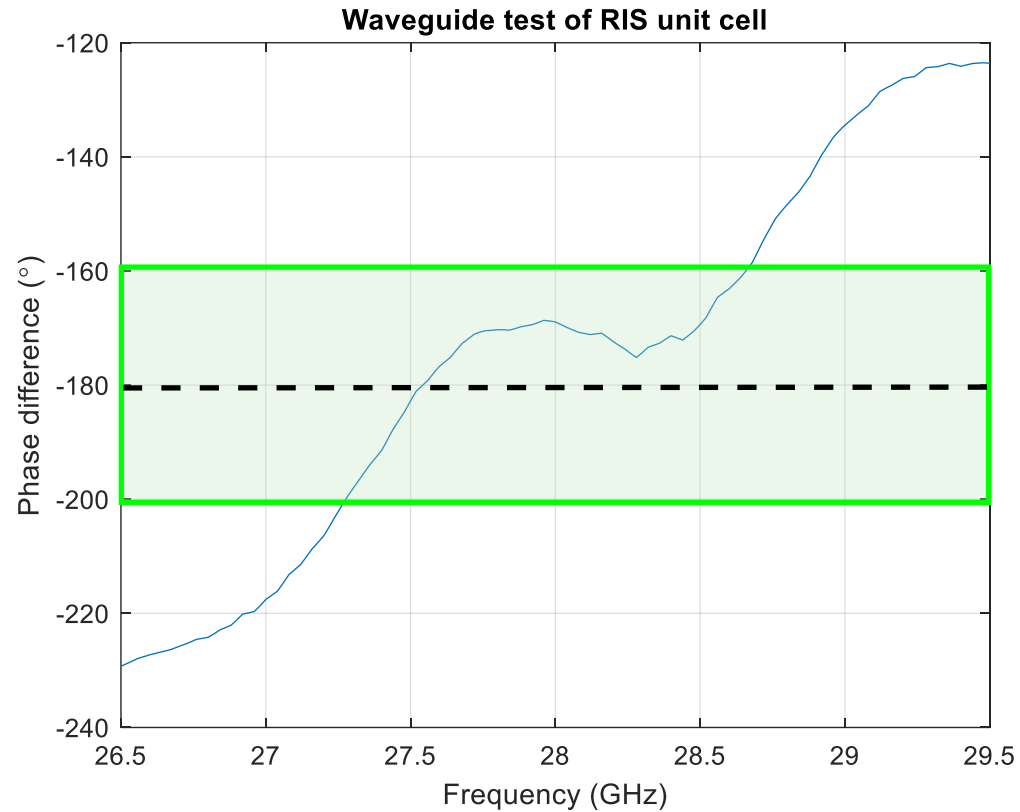


WR-28 waveguides have a rectangular cross-section
 Width (a-dimension): 7.112 mm
 Height (b-dimension): 3.556 mm

WR-28 → 10mmx5mm tapered transition

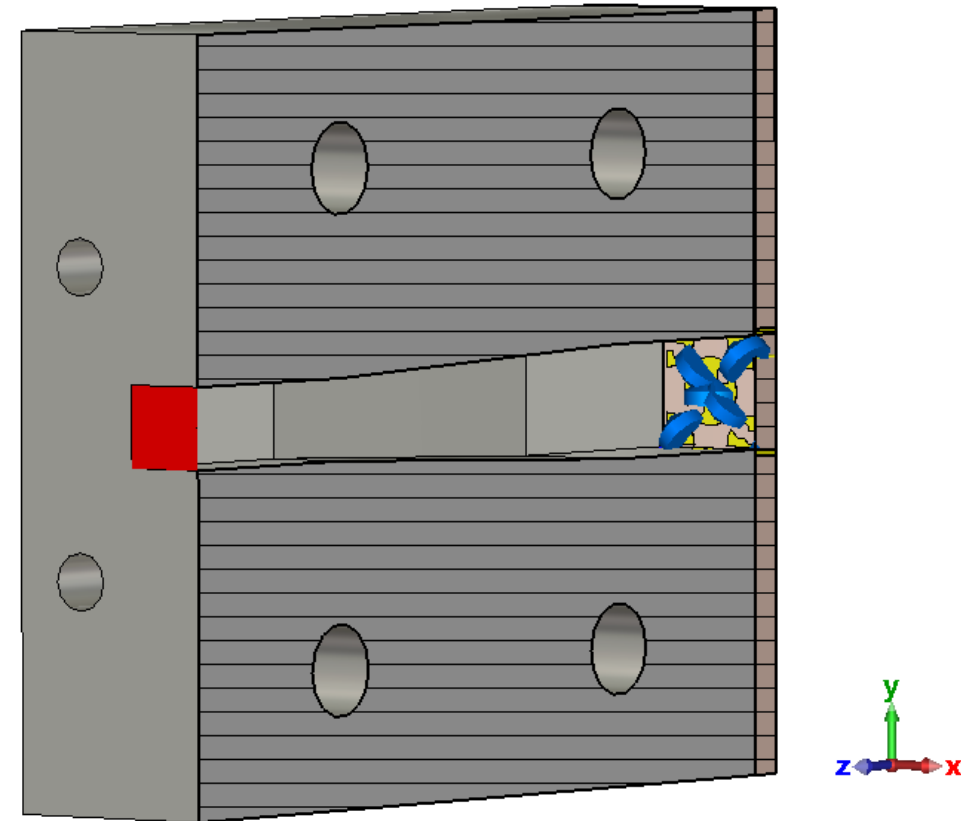
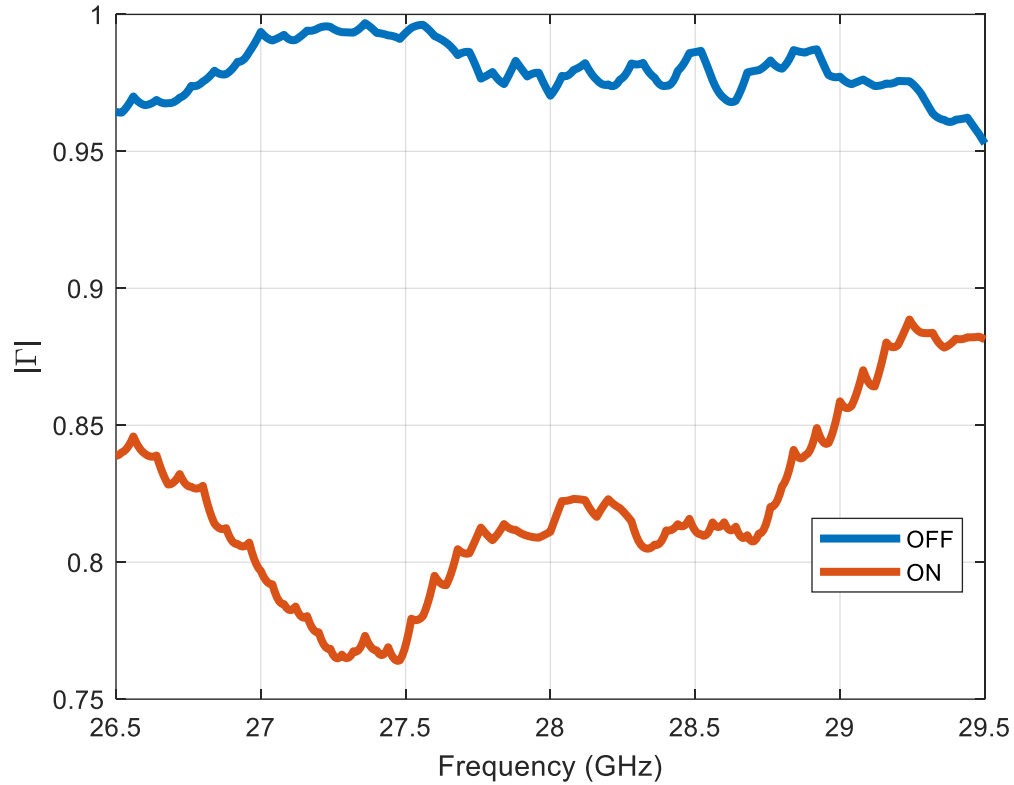
The geometry of the scattering element is the same as in RIS modelling, yet periodicity is slightly changed to fit into the waveguide

Waveguide test phase difference



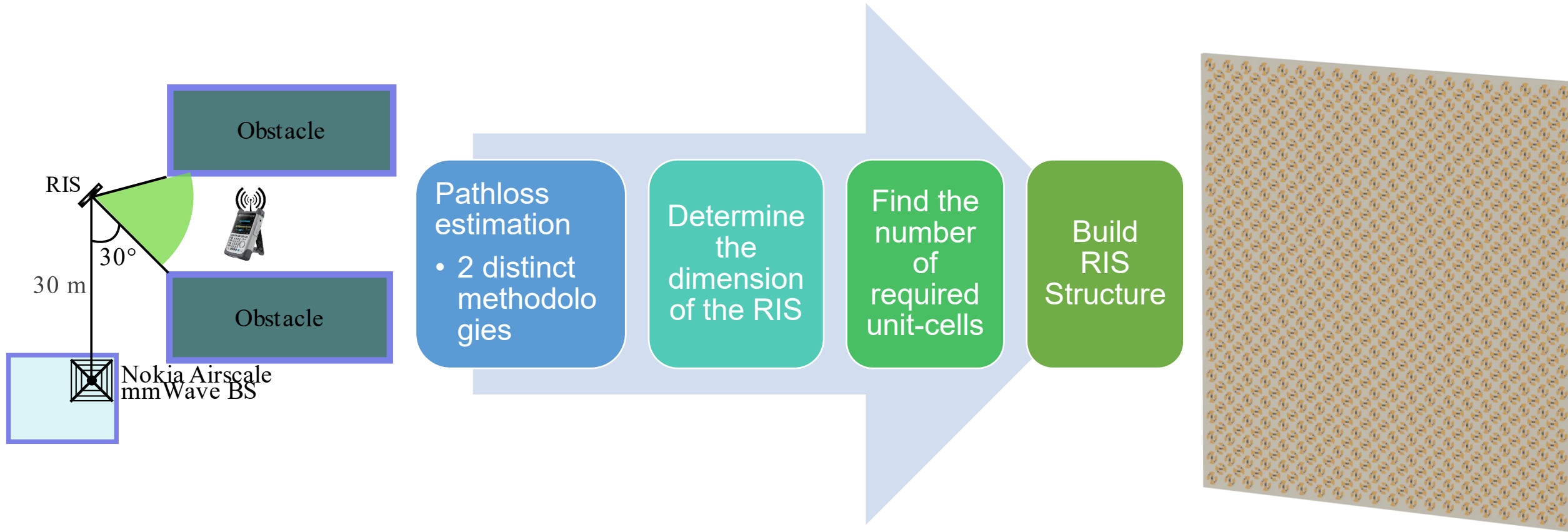
WR-28 → 10mmx5mm tapered transition

Waveguide test amplitude



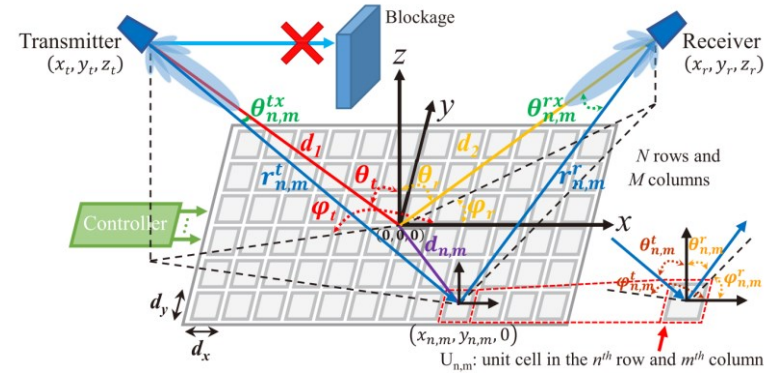
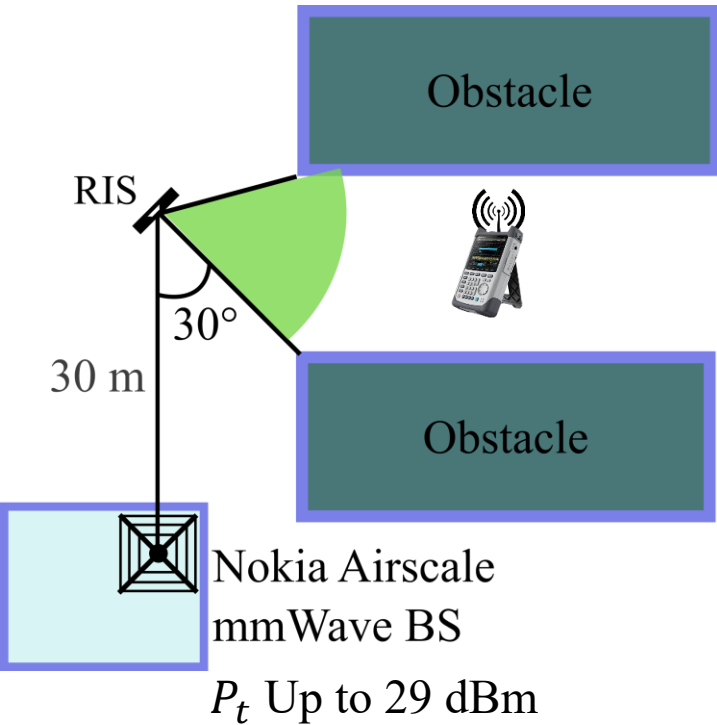
WR-28 → 10mmx5mm tapered transition

Full RIS simulations



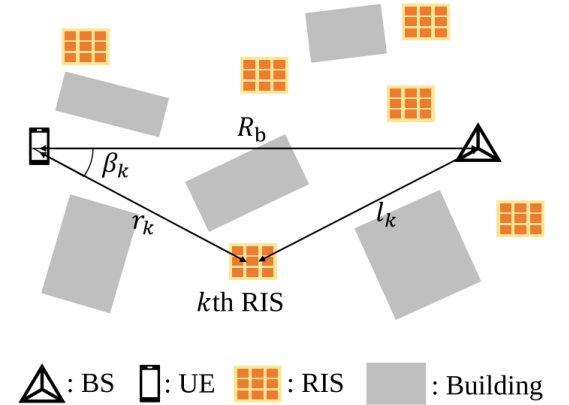
Full RIS Simulation

Pathloss models



$$\begin{aligned}
 PL_{general}^{refined} &= \frac{P_t}{P_r} \\
 &= \frac{16\pi^2}{G_t G_r (d_x d_y)^2} \\
 &\quad \times \frac{1}{\left| \sum_{m=1}^M \sum_{n=1}^N \frac{\sqrt{F_{n,m}^{combine}} \Gamma_{n,m}}{r_{n,m}^t r_{n,m}^r} e^{-\frac{j2\pi(r_{n,m}^t + r_{n,m}^r)}{\lambda}} \right|^2}
 \end{aligned}$$

[1] W. Tang et al., "Path Loss Modeling and Measurements for Reconfigurable Intelligent Surfaces in the Millimeter-Wave Frequency Band," in IEEE Transactions on Communications, vol. 70, no. 9, pp. 6259-6276, Sept. 2022, doi: 10.1109/TCOMM.2022.3193400.

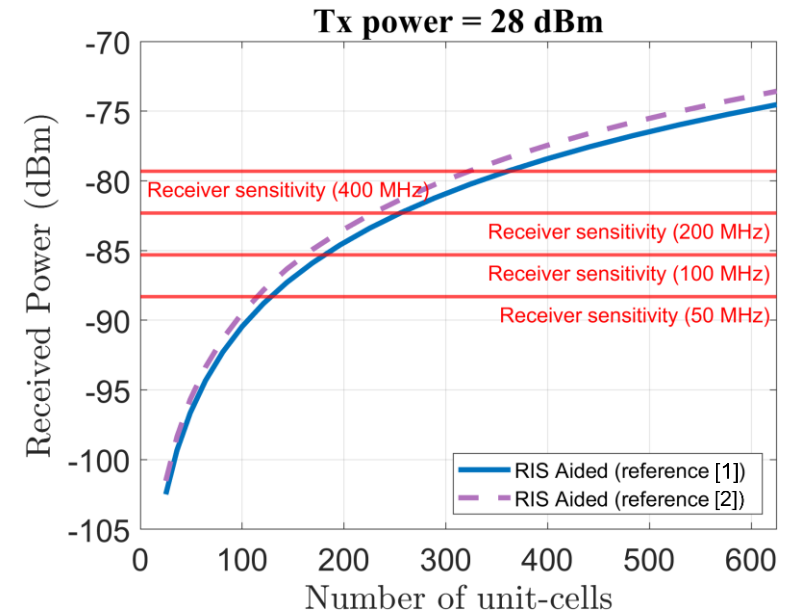
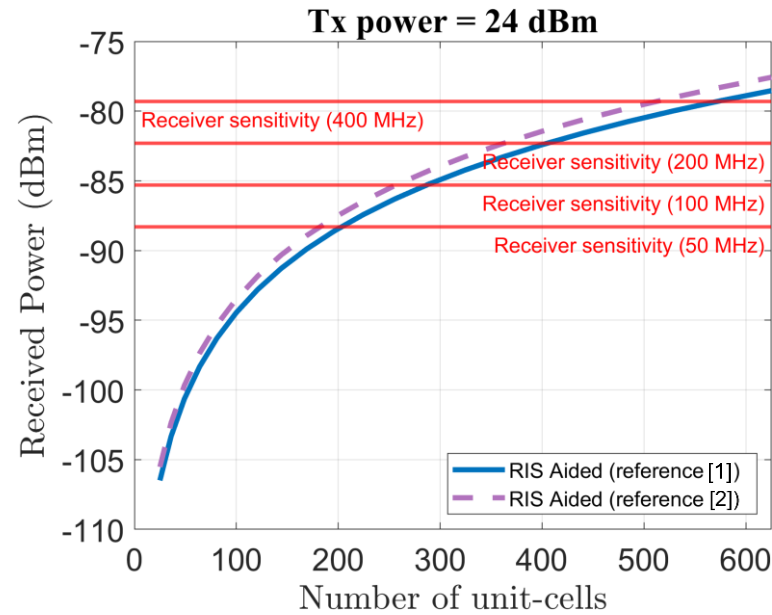
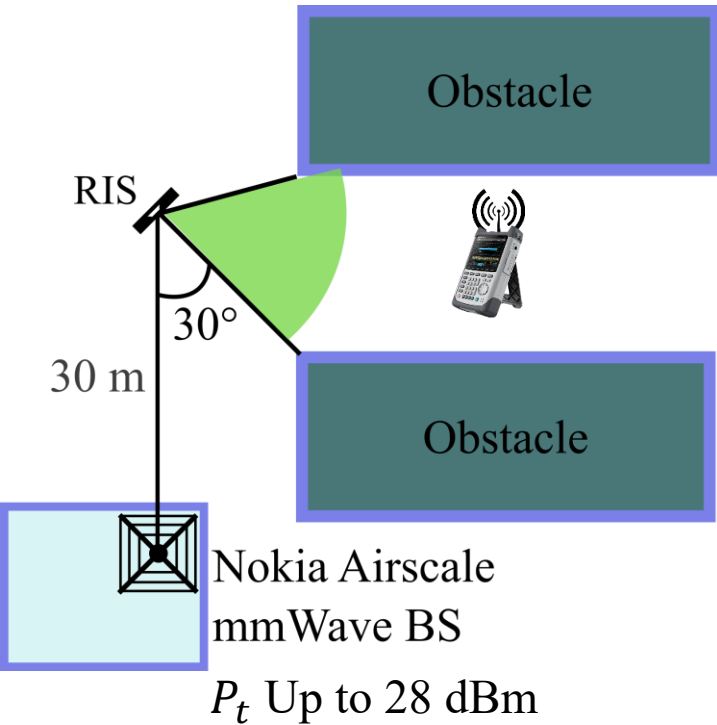


$$P_{rr} = \frac{P_t N_t^2 G_t M_d^2 N_d^2 l_u^2 \mu^2 \rho^2}{64\pi^3 (\tilde{l}_k \tilde{r}_k)^\alpha},$$

[2] Z. Li, H. Hu, J. Zhang and J. Zhang, "RIS-Assisted mmWave Networks With Random Blockages: Fewer Large RISs or More Small RISs?," in IEEE Transactions on Wireless Communications, vol. 22, no. 2, pp. 986-1000, Feb. 2023, doi: 10.1109/TWC.2022.3200157.

Full RIS Simulation

Determining the number of Unit-cells



[1] W. Tang et al., "Path Loss Modeling and Measurements for Reconfigurable Intelligent Surfaces in the Millimeter-Wave Frequency Band," in IEEE Transactions on Communications, vol. 70, no. 9, pp. 6259-6276, Sept. 2022, doi: 10.1109/TCOMM.2022.3193400.

[2] Z. Li, H. Hu, J. Zhang and J. Zhang, "RIS-Assisted mmWave Networks With Random Blockages: Fewer Large RISs or More Small RISs?," in IEEE Transactions on Wireless Communications, vol. 22, no. 2, pp. 986-1000, Feb. 2023, doi: 10.1109/TWC.2022.3200157.

$f_0 = 27.275$ GHz, $P_x = P_y = 4.6$ mm – 30 meters
 $G_t = 29$ dBi, $G_r = 2$ dBi

Table 7.3.2.3-1: Reference sensitivity

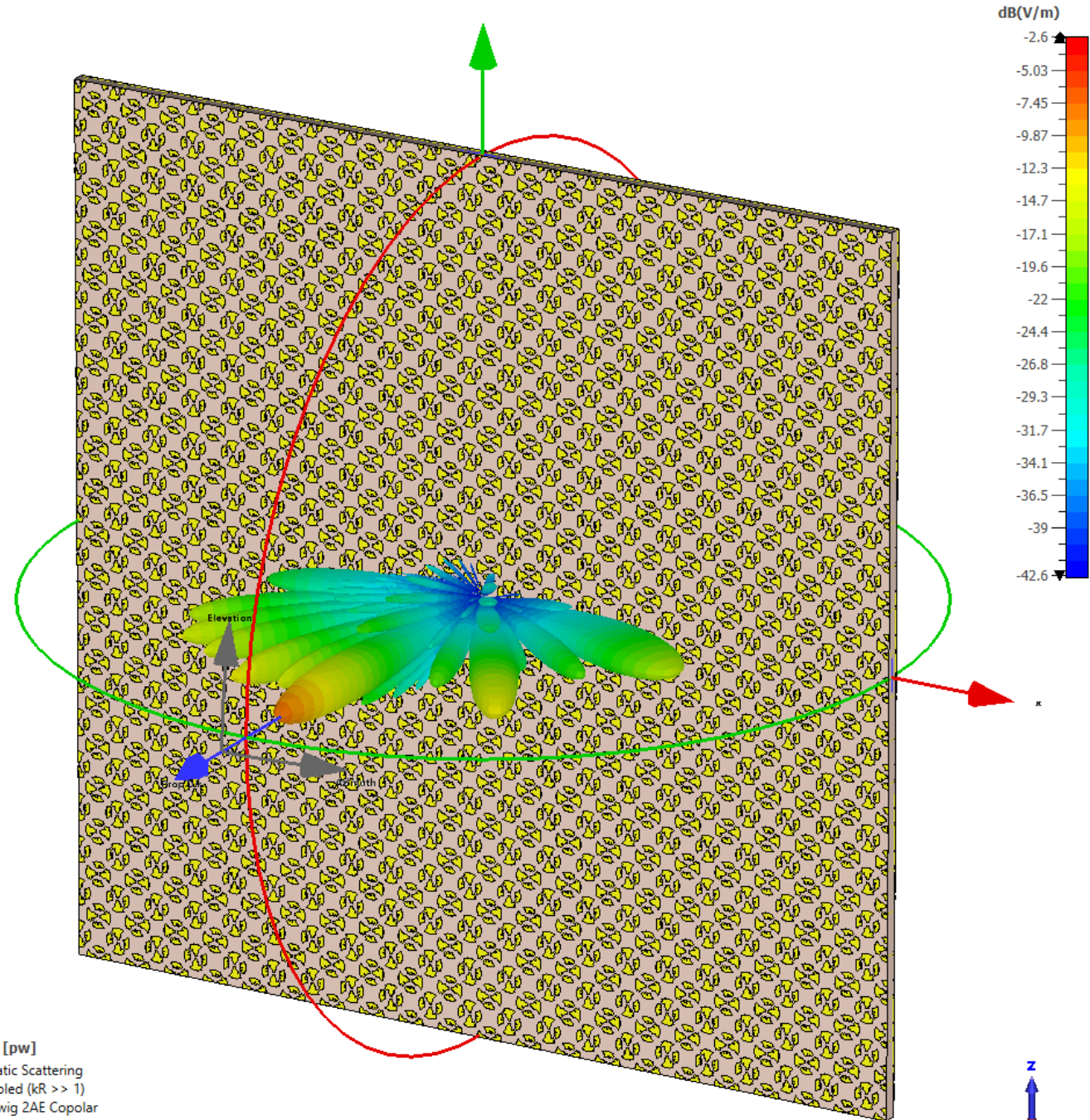
Operating band	REFSENS (dBm) / Channel bandwidth			
	50 MHz	100 MHz	200 MHz	400 MHz
n257	-88.3	-85.3	-82.3	-79.3
n258	-88.3	-85.3	-82.3	-79.3
n260	-85.7	-82.7	-79.7	-76.7
n261	-88.3	-85.3	-82.3	-79.3

NOTE 1: The transmitter shall be set to P_{UMAX} as defined in clause 6.2.4

Full RIS Simulation

Numerical results

-30° Incidence
+0° reflection
Co-polar



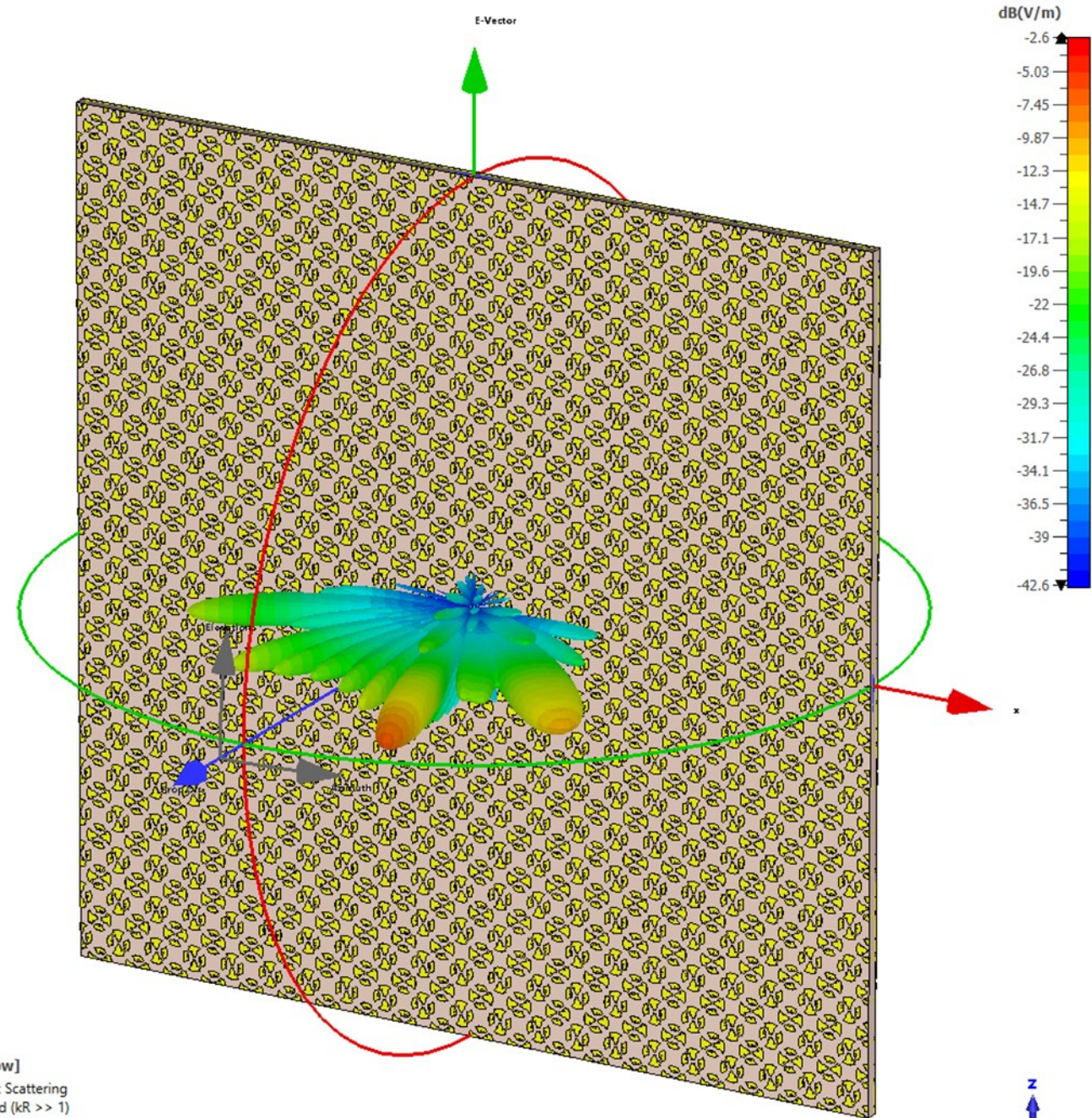
farfield (f=27.275) [pw]

Type	Bistatic Scattering
Approximation	enabled (kR >> 1)
Component	Ludwig 2AE Copolar
Output	E-Field(r=1m)
Frequency	27.275 GHz
E _{max} (Abs)	-1.959 dB(V/m)
E _{max} (Copolar)	-1.959 dB(V/m)

Full RIS Simulation

Numerical results

–30° Incidence
 +45° reflection
 Co-polar



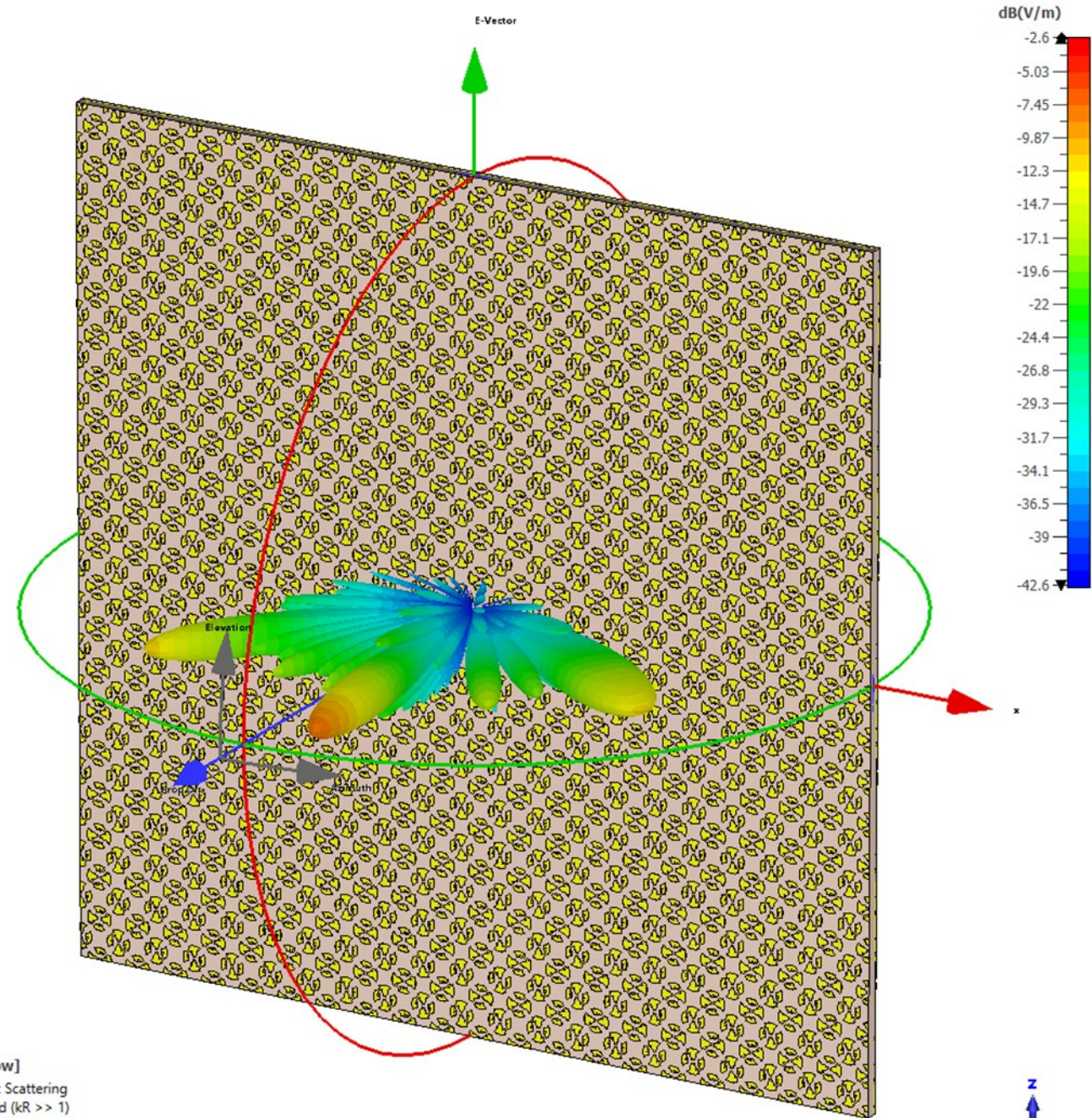
farfield (f=27.275) [pw]

Type	Bistatic Scattering
Approximation	enabled (kR >> 1)
Component	Ludwig 2AE Copolar
Output	E-Field(r=1m)
Frequency	27.275 GHz
E _{max} (Abs)	-2.115 dB(V/m)
E _{max} (Copolar)	-2.115 dB(V/m)

Full RIS Simulation

Numerical results

-30° Incidence
+60° reflection
Co-polar

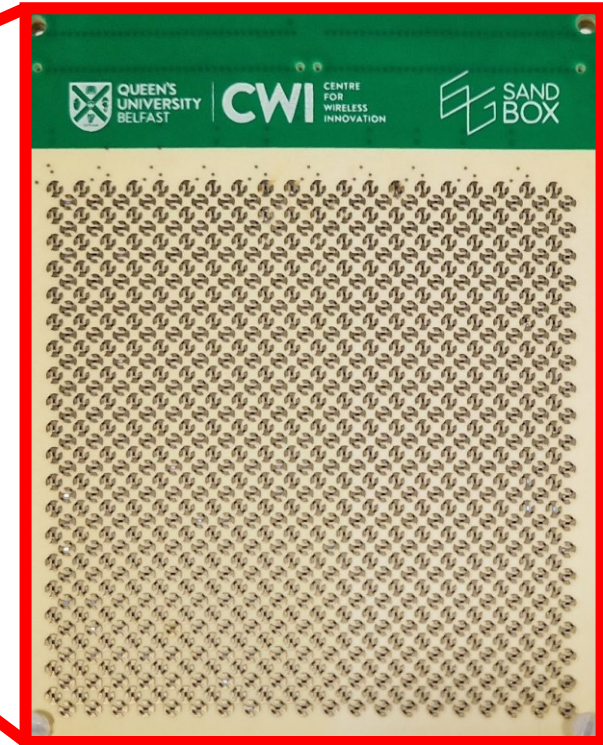
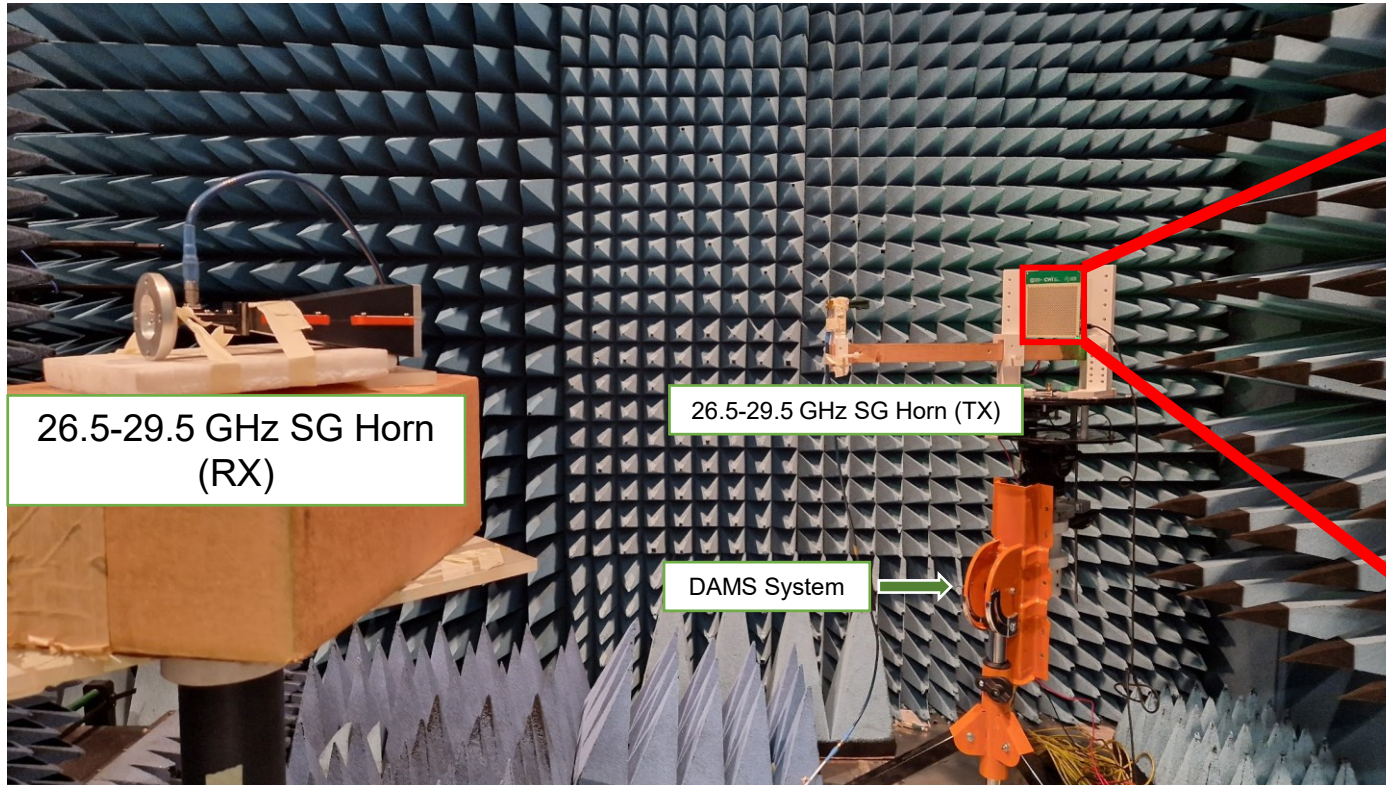


farfield (f=27.275) [pw]

Type	Bistatic Scattering
Approximation	enabled (kR >> 1)
Component	Ludwig 2AE Copolar
Output	E-Field(r=1m)
Frequency	27.275 GHz
Emax (Abs)	-2.044 dB(V/m)
Emax (Copolar)	-2.044 dB(V/m)

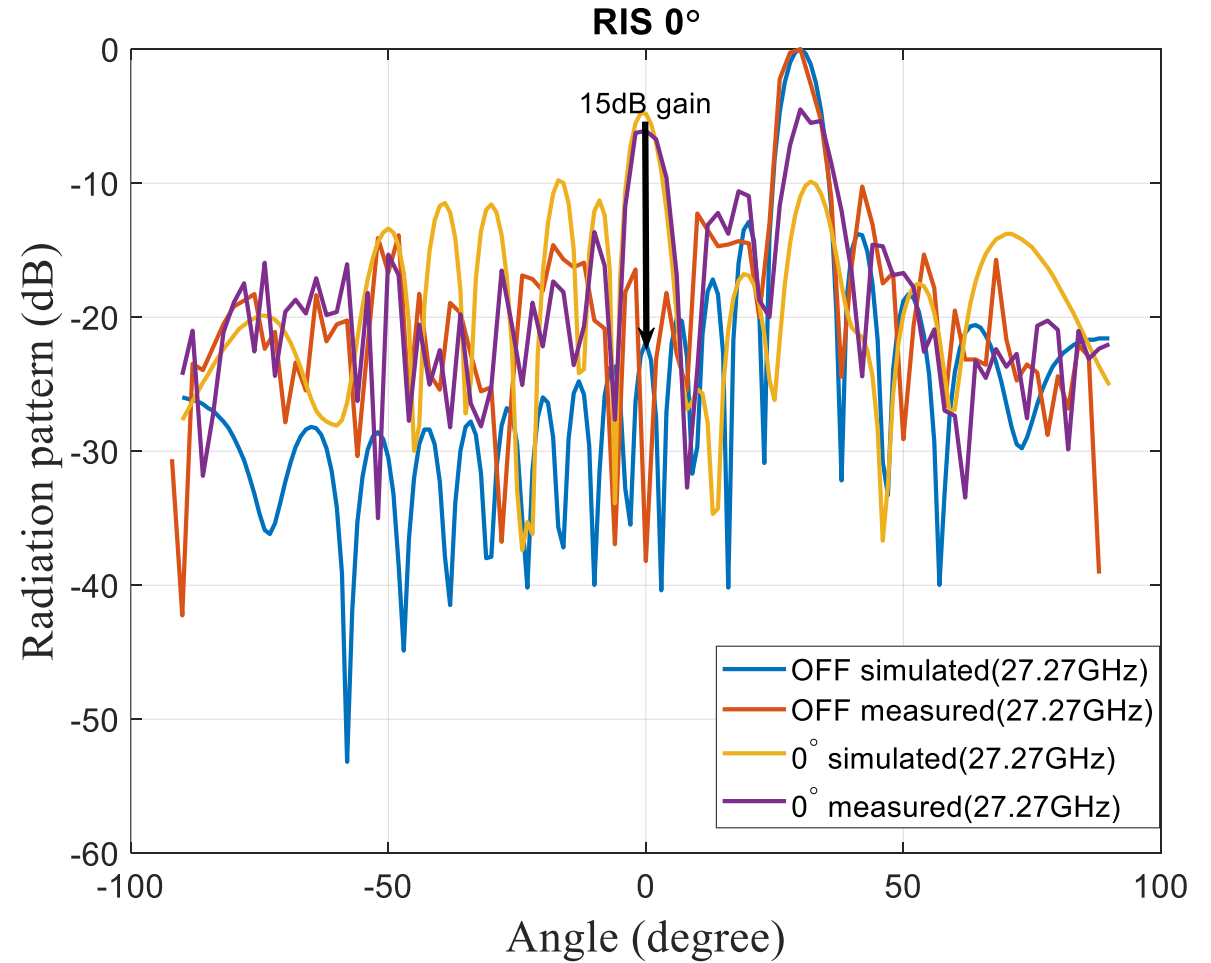
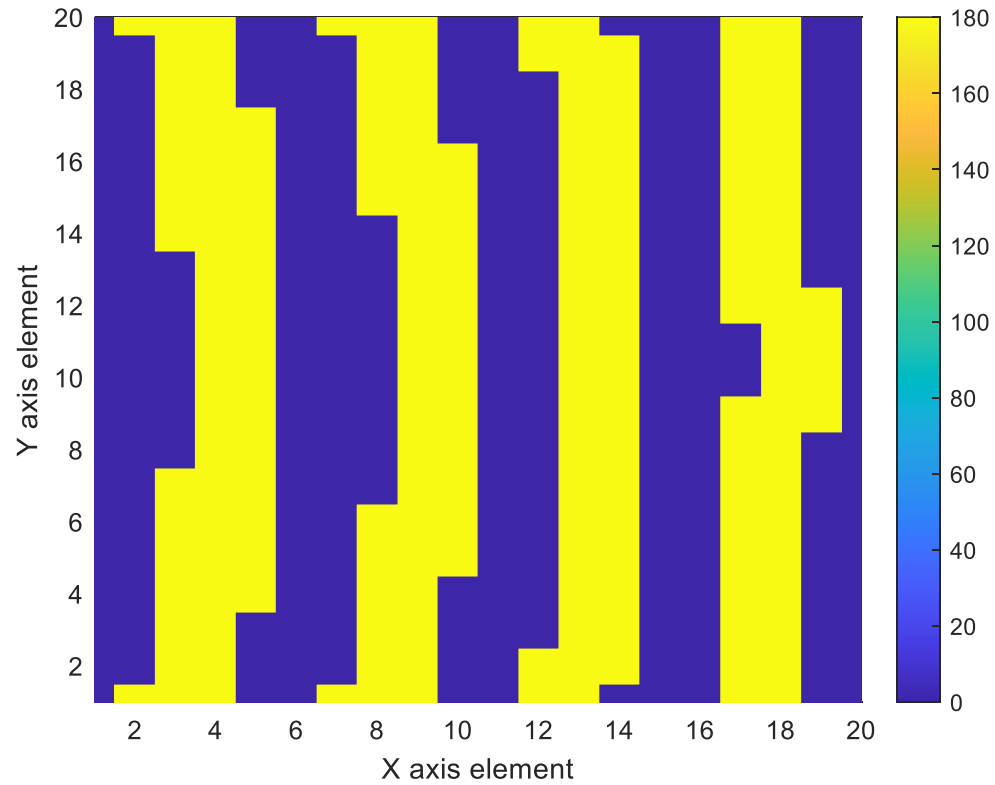
Experimental Results

Set-up



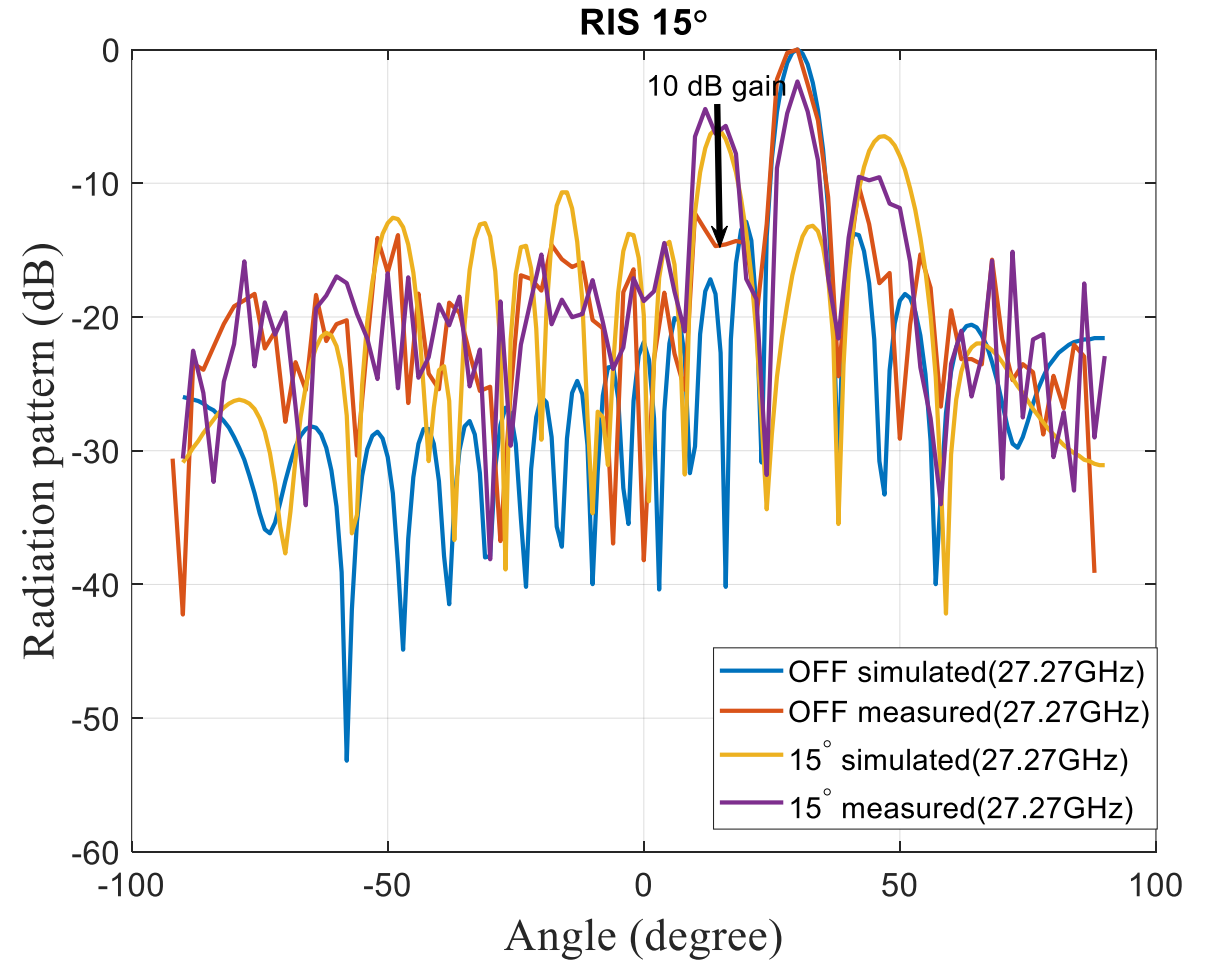
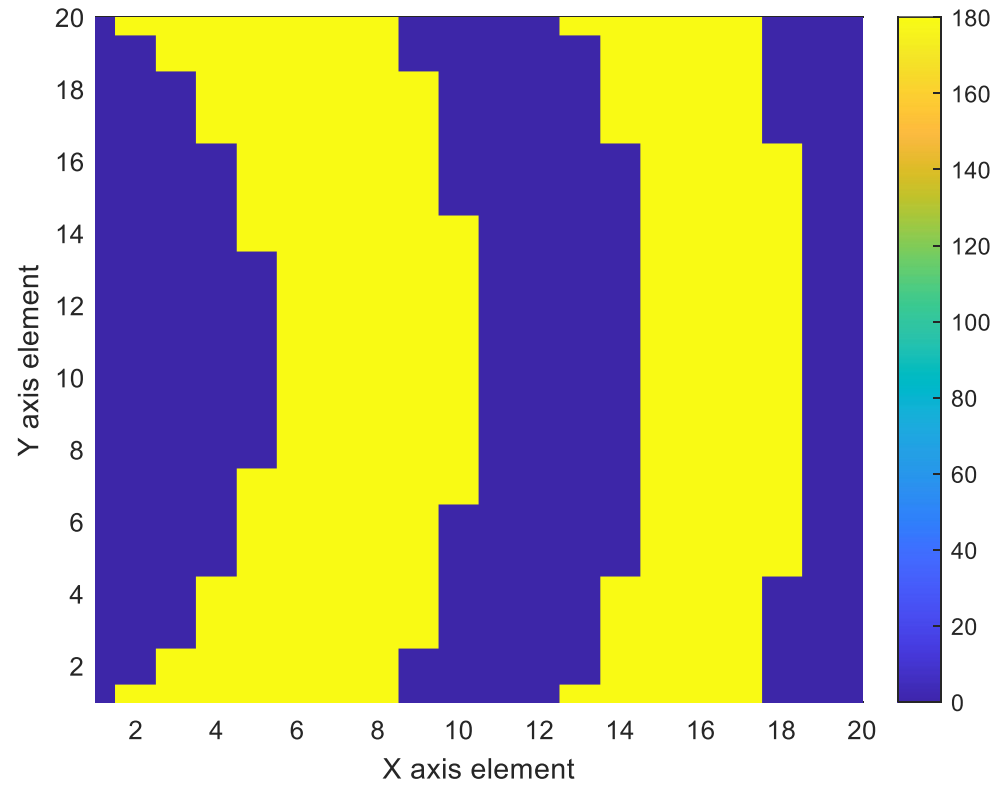
Experimental Results

0 degree direction



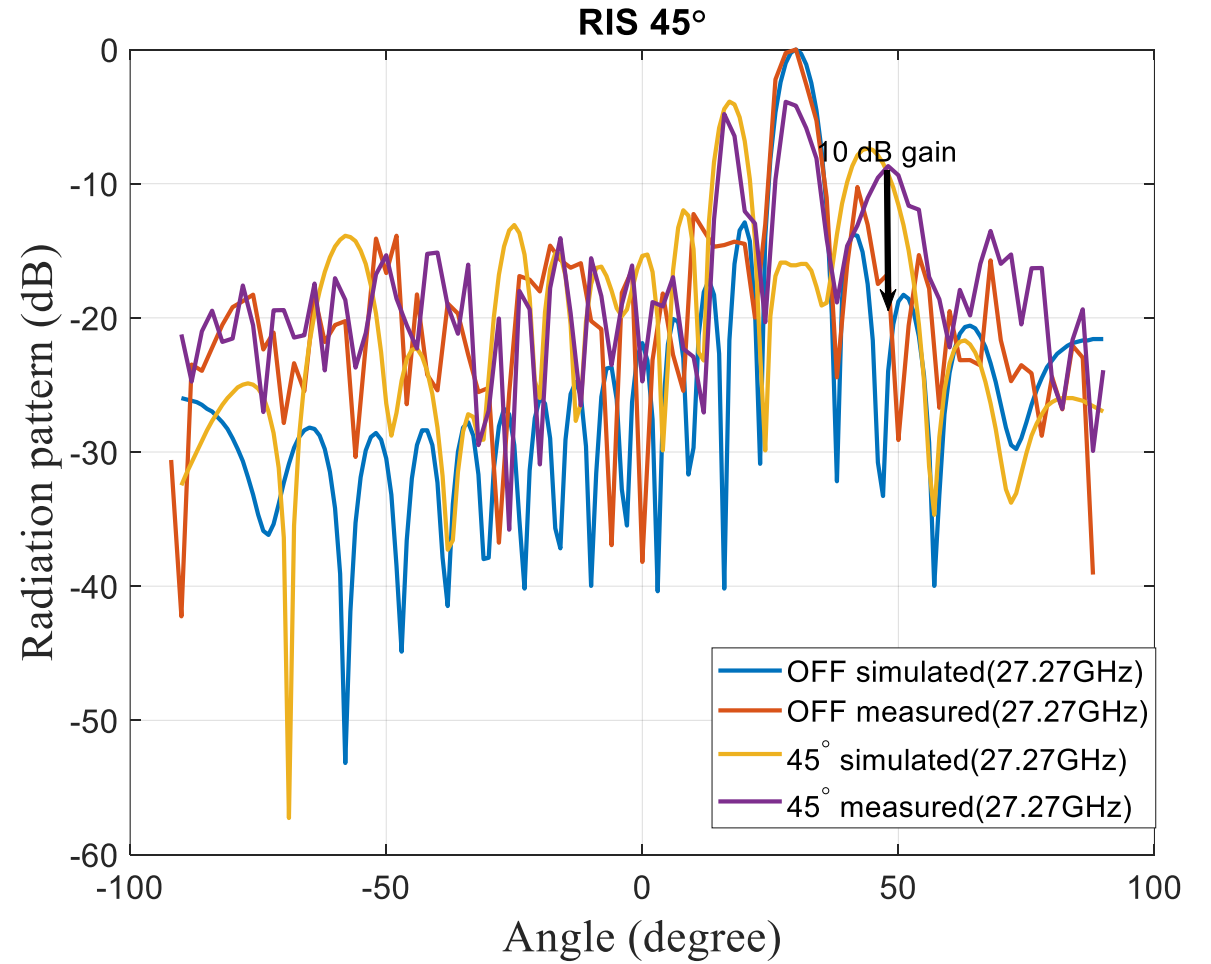
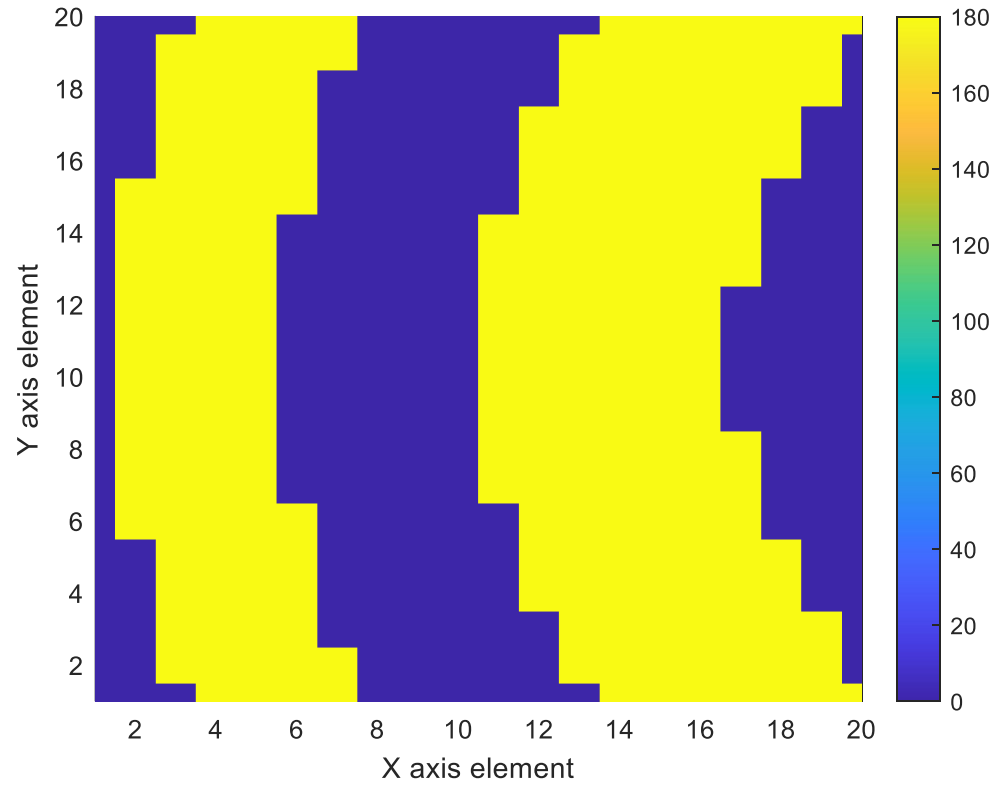
Experimental Results

15 degree direction



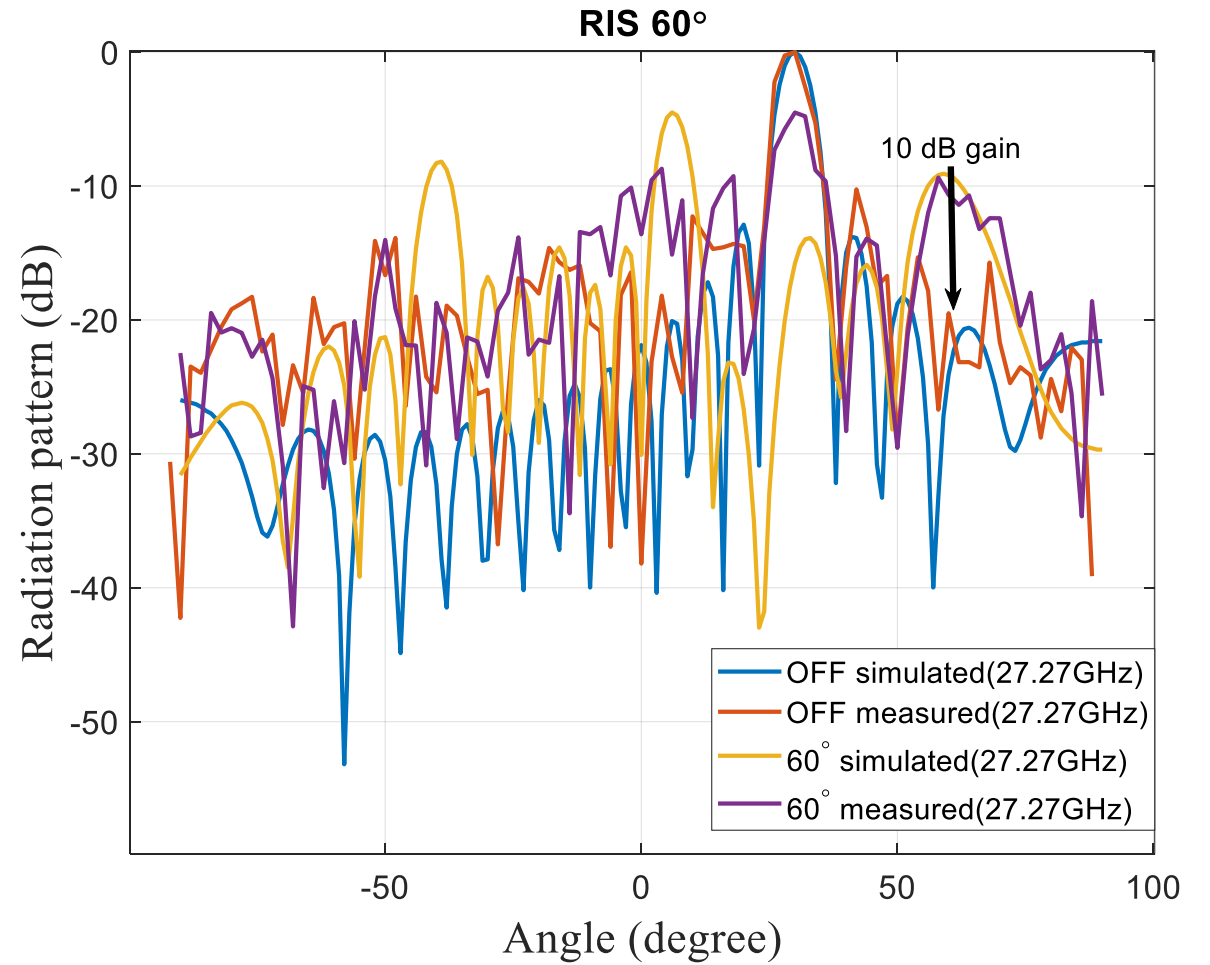
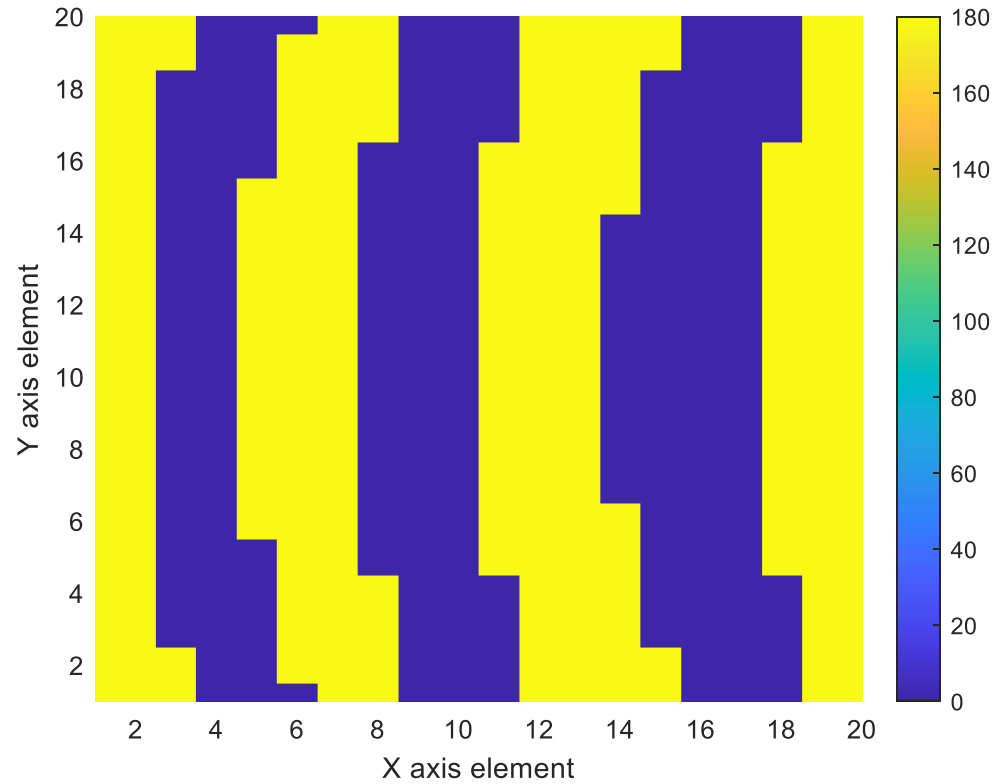
Experimental Results

45 degree direction



Experimental Results

60 degree direction



Conclusions

A novel unit-cell for RIS has been presented

Coverage of the entire n257 5G mmWave band

Final dimensions obtained based on the scenario it will be used

- Considered 2 pathloss models

Simulations of the full RIS show specular reflection and some grating lobes

- Quantization
- Spacing between unit-cells to provide dual-polarization capability

Initial measurement stages

- Needs refinement
- Results are encouraging

